Vol. 621: 169–184, 2019
https://doi.org/10.3354/meps12995

MARINE ECOLOGY PROGRESS SERIES
Mar Ecol Prog Ser

Published July 4

Movement and residency patterns of reef manta rays *Mobula alfredi* in the Amirante Islands, Seychelles

Lauren R. Peel[1,2,3,4,*], Guy M. W. Stevens[3], Ryan Daly[4,5], Clare A. Keating Daly[4], James S. E. Lea[6,7], Christopher R. Clarke[7], Shaun P. Collin[1,8], Mark G. Meekan[2]

[1]School of Biological Sciences, The Oceans Institute and The Oceans Graduate School, The University of Western Australia, Crawley, Western Australia 6009, Australia

[2]The Australian Institute of Marine Science, Crawley, Western Australia 6009, Australia

[3]The Manta Trust, Catemwood House, Norwood Lane, Corscombe, Dorset DT2 0NT, UK

[4]Save Our Seas Foundation – D'Arros Research Centre (SOSF-DRC), Rue Philippe Plantamour 20, 1201 Genève, Switzerland

[5]South African Institute for Aquatic Biodiversity (SAIAB), Private Bag 1015, Grahamstown 6140, South Africa

[6]Department of Zoology, University of Cambridge, Cambridge CB2 1TN, UK

[7]Marine Research Facility, Jeddah 21443, Saudi Arabia

[8]School of Life Sciences, La Trobe University, Bundoora, Victoria 3086, Australia

ABSTRACT: Reef manta rays *Mobula alfredi* are large filter-feeding elasmobranchs that are undergoing substantial population declines on a global scale. In order to effectively conserve and manage populations, it is crucial that the drivers of their occurrence are defined and that key aggregation areas for this species are identified and protected. Here, we used passive acoustic telemetry to monitor and assess the movement ecology of *M. alfredi* in the remote Amirante Islands, Republic of Seychelles. Acoustic transmitters were externally deployed on *M. alfredi* at D'Arros Island (n = 42) and movement data retrieved from an array of 70 acoustic receivers deployed throughout the Amirantes between November 2013 and October 2017. Individuals were detected year-round, with a peak in detections occurring between November and April coinciding with the arrival and departure of the north-west monsoon. Individuals were most likely to be detected within the array during the day, at low wind speeds, and when water temperatures were approximately 28°C. Additionally, individuals were more likely to be detected during a new moon, when the tidal range was at its highest, and on the slack of high tide. *M. alfredi* travelled widely within the Amirantes, with larger individuals travelling greater distances per day than smaller individuals and juveniles. The majority of detections (89%) were recorded within 2.5 km of the shoreline of D'Arros Island and the neighbouring St. Joseph Atoll, highlighting the importance of these sites to *M. alfredi* in the Amirante Islands, and supporting the proposed development of a marine protected area at this location.

KEY WORDS: Acoustic telemetry · Residency · Site fidelity · Environmental drivers · Elasmobranch · Conservation

1. INTRODUCTION

Reef manta rays *Mobula alfredi* (Marshall et al. 2009, White et al. 2017) are large planktivorous elasmobranchs of the family Mobulidae (the devil rays; Notarbartolo-di-Sciara 1987, Couturier et al. 2012, White et al. 2017). Conservative life history strategies are characteristic of this group, with the majority of species exhibiting slow growth rates, late maturity and low fecundity (Couturier et al. 2012, Lawson et al. 2017, Stewart et al. 2018a). These reproductive traits greatly increase the susceptibility of mobulid popula-

*Corresponding author: lauren.peel@research.uwa.edu.au

tions to local and broad-scale extinctions resulting from unsustainable fishing pressures, and minimise the rate at which populations can recover from loss (Holden 1974, Musick et al. 2000, Dulvy et al. 2014).

Targeted fishing practices aiming to supply mobulid gill plates to the market for traditional Asian medicine have resulted in the decline of *M. alfredi* populations on a global scale in recent decades (Ward-Paige et al. 2013, Whitcraft et al. 2014, Lawson et al. 2017, O'Malley et al. 2017). This is particularly notable in the Indian Ocean, where 3 of the 5 most intensive fisheries for mobulids in the world are located (Sri Lanka, India and Indonesia; Heinrichs et al. 2011). The by-catch of mobulids in the fishing gear of other fisheries contributes additional pressures to these populations, with individuals becoming entangled in gill and purse-seine nets (Rohner et al. 2017, Temple et al. 2019). Given that mobulid fisheries have now been identified in Mozambique (Heinrichs et al. 2011, Dent & Clarke 2015), and mobulid landings by small-scale fisheries are reported in Pakistan (Moazzam 2018) and throughout eastern Africa (Kenya, Mauritius and Tanzania; Temple et al. 2018), there is an urgent need to identify and protect key aggregation areas for *M. alfredi* in the Western Indian Ocean (WIO) to ensure the conservation of their populations.

Marine protected areas (MPAs) provide a relatively simple, regional-scale conservation and management strategy for populations of *M. alfredi* (Graham et al. 2012, Stewart et al. 2016, Couturier et al. 2018) that complement international efforts to restrict their global trade (listing on CITES Appendix II; Marshall et al. 2018). In addition to preventing targeted fishing efforts towards this 'Vulnerable' species (IUCN Red List of Threatened Species; Marshall et al. 2018), MPAs also serve to reduce the risk of by-catch, accidental entanglement and boat strikes to individuals (Heinrichs et al. 2011, Moazzam 2018, Stewart et al. 2018a). By specifically targeting key aggregation sites for *M. alfredi*, MPAs are able to direct resources and effort to places where populations will most greatly benefit from protection (Kessel et al. 2017, Lawson et al. 2017). However, the successful design and implementation of MPAs relies on an understanding of the movement and residency patterns of target species, and it is for this reason that an increasing number of studies focussing on the ecology of manta rays have incorporated an element of animal tracking using telemetry (Dewar et al. 2008, Deakos et al. 2011, Braun et al. 2014, Jaine et al. 2014, Stewart et al. 2016, 2018a, Kessel et al. 2017).

Passive acoustic telemetry is a popular tool for the assessment of movement and connectivity patterns of populations of *M. alfredi* because it is cost effective, allows collection of records of individual movements for up to a decade and can be implemented in remote locations (Hussey et al. 2015, Stewart et al. 2018a). Such studies of *M. alfredi* in Hawaii (Clark 2010), Palmyra Atoll (McCauley et al. 2014), the Red Sea (Braun et al. 2015), eastern Australia (Couturier et al. 2018) and Indonesia (Setyawan et al. 2018) have emphasised the typically coastal and limited nature of the movement patterns of this species, which displays high levels of residency and site fidelity. Little information is currently available about the movement ecology of *M. alfredi* in the WIO, where numerous populations exist, but are afforded little to no national-scale protection from commercial or artisanal fisheries (Marshall et al. 2011, Temple et al. 2018).

Here, we used passive acoustic telemetry to investigate the presence and movement patterns of *M. alfredi* in the Amirante Islands in the Republic of Seychelles. Little is currently known about the movement ecology of *M. alfredi* within this region of the WIO, as the islands and atolls around which they aggregate are often remote and difficult to access. The lack of an established manta fishery in Seychelles — despite records of historic fishing practices and occasional landings of by-catch (Keynes 1959, Temple et al. 2018) — is also significant, as it provides an opportunity for our study to assess the movement and residency patterns of *M. alfredi* at a locality where there is likely little to no targeted fishing at present, but where increasing market demand may occur in the future (Temple et al. 2018). Telemetry data were used to examine patterns of residency and site fidelity of *M. alfredi* throughout the Amirante Islands, and to investigate how the observed patterns varied with the sex and maturity status of tagged individuals. Trends in patterns of occurrence with respect to environmental, temporal and biological variables were also examined. Finally, detection data were used to assess the potential benefits of a proposed MPA at D'Arros Island and St. Joseph Atoll to *M. alfredi* within the Amirante Islands, and the significance of this location to a globally vulnerable species currently afforded no national-scale protection in Seychelles (Temple et al. 2018).

2. MATERIALS AND METHODS

2.1. Study site

The Republic of Seychelles is an archipelago of 115 islands located in the tropical WIO (Fig. 1A). Two seasons (monsoons) shape the climate of the nation,

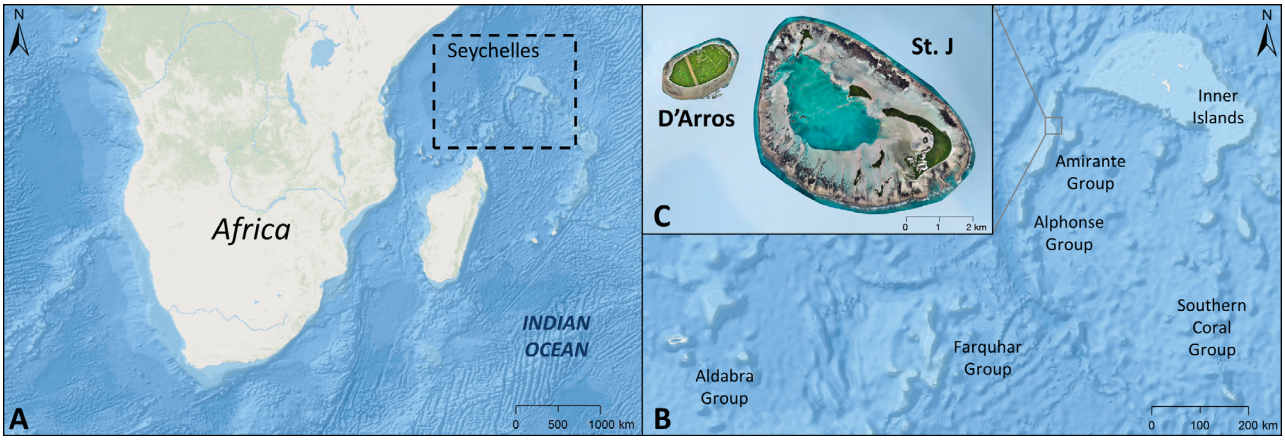

Fig. 1. (A) Western Indian Ocean. The dashed square outlines the location of (B) Republic of Seychelles, an archipelago of 115 islands. The Amirante Island Group, located upon the Amirantes Bank, is 1 of 6 island groups identified within the country. (C) Reef manta rays *Mobula alfredi* aggregate in the Amirantes at D'Arros Island and St. Joseph Atoll (St. J), the focal site for this acoustic telemetry study. Maps created in ArcGIS 10.3 (www.esri.com/) using GEBCO_08 (version 20100927) bathymetry data. Satellite imagery © Save Our Seas Foundation

with the lighter and less-persistent winds of the wet north-west monsoon blowing from March to October, and the stronger, steadier south-easterly winds of the dry south-east monsoon, prevailing from April through September (Schott & McCreary 2001, Komdeur & Daan 2005). Despite encompassing an exclusive economic zone of 1.4 million km^2, the total land mass of Seychelles covers just 459 km^2. Given the sparse distribution of islands throughout the region, each is therefore considered to fall within 1 of 6 discrete island groups based on its geography (Fig. 1B; Stoddart et al. 1979).

The focal area for our study was the Amirante Island Group, a cluster of 24 small islands and islets located on the Amirantes Bank approximately 250 km south-west of the capital, Victoria, and extending over a distance of approximately 152 km (Hamylton et al. 2012). On the Bank, water depths reach a maximum of 70 m in the centre before rising to a shallower outer rim of 11 to 27 m, and then steeply dropping to depths greater than 1000 m (Hamylton et al. 2012).

D'Arros Island (5° 24.9' S, 53° 17.9' E) is a small (1.71 km^2) coralline island located midway along the Amirantes Bank within the Amirante Islands, neighboured closely to the east by St. Joseph Atoll (Fig. 1C). These 2 land masses are surrounded by insular platform reefs and sea grass beds, and are separated by a 1 km wide channel that reaches a depth of 60 m in the centre (Stoddart et al. 1979). *Mobula alfredi* have been observed to aggregate nearly year-round at this location, and for this reason it was chosen as the focal site for this study within the Amirante Islands.

2.2. Tag deployment

Acoustic tags (Vemco; n = 42) were externally deployed on *M. alfredi* at D'Arros Island across 2 tagging periods; November 2013–March 2014 (Period One; n = 20) and November 2016 (Period Two; n = 22). All tags deployed in Period One were V16-5H tags, and during Period Two, 13 V16-5H and 9 V16TP-5H (temperature and depth sensor tags) were deployed. Tag anchors were made of either titanium (n = 15) or stainless steel (n = 27), and all were of a similar design to the large titanium anchor (Wildlife Computers). Tags were deployed *in situ* using a modified Hawaiian sling, and positioned towards the posterior dorsal surface of each manta ray such that the tag was not trailing over the back edge of the pectoral fin and the anchor would not pose a risk to the body cavity of the individual. All tagged animals were photographed and identified prior to being tagged, and their size and sex recorded with the tag ID number. Individuals were identified from the unique pattern of pigmentation on their ventral surface, which does not vary throughout their lifetime (Marshall et al. 2009, 2011, Couturier et al. 2014, Germanov & Marshall 2014). The sex of each tagged individual was assigned based on the observed presence (males) or absence (females) of claspers (Marshall et al. 2009). Wingspan was estimated visually to the nearest 0.1 m and used as a proxy to estimate maturity status. Where possible, estimated wing span measurements were verified using a diver-operated stereo-video camera system (Letessier et al. 2015). This system consisted of 2 GoPro Hero4 Silver edition

cameras mounted 70 cm apart on a base bar inwardly converged at 6°, and individual wing spans were measured from wing-tip to wing-tip using the program EventMeasure (SeaGIS). Individuals were classified into 1 of the following 3 'life stage' groups based on their estimated size: juvenile (any individual ≤2.4 m), sub-adult (male: 2.5–2.8 m; female: 2.5–3.1 m) or adult (male: ≥2.9 m; female: ≥3.2 m; Deakos 2012, Stevens 2016). The presence of mating scars (females only) and degree of calcification of the claspers (males only) were also considered during assignment of maturity status.

2.3. Acoustic receiver array

An array of 70 acoustic receivers (model VR2W; Vemco) were deployed around the islands of the Amirante Group between 2012 and 2016. A large proportion of the receivers (n = 32, 46%) were positioned within 2.5 km of the shorelines of D'Arros Island and St. Joseph Atoll, with the remaining receivers located around other islands of the Amirantes, or at key locations across the bank (Fig. 2). Detections of tagged *M. alfredi* were recorded and monitored between November 2013 and October 2017. Deployed tags were detected within approximately 150 m of the receivers as determined by preliminary range testing (mean = 165 ± 33 m; Lea et al. 2016). Data from receivers in close proximity to D'Arros Island were downloaded every 6 mo, with offshore receivers being downloaded annually each November to coincide with calm weather conditions. Once a year, the battery of each receiver was replaced and the receiver inspected for damage or clock drift. Upon import of the detection data into a Microsoft Access database, false positive detections were removed through filtration for active tag IDs, and any receiver clock-drift time corrections were calculated assuming linear drift (Lea et al. 2016). Four tags were removed from the dataset prior to analysis because they were lost from individuals within 1 wk. Tag loss was confirmed through resightings of these individuals. Detection data for the remaining tags were examined visually to ensure that tags had not been shed within range of any receivers. Where continuous detections were recorded for a tag at a single receiver over a long period of time (>24 h), the tag was assumed to have fallen from the animal, and detection data from that receiver were subsequently removed from the dataset prior to analysis. For all analyses, values of the standard deviation are presented with means unless otherwise stated.

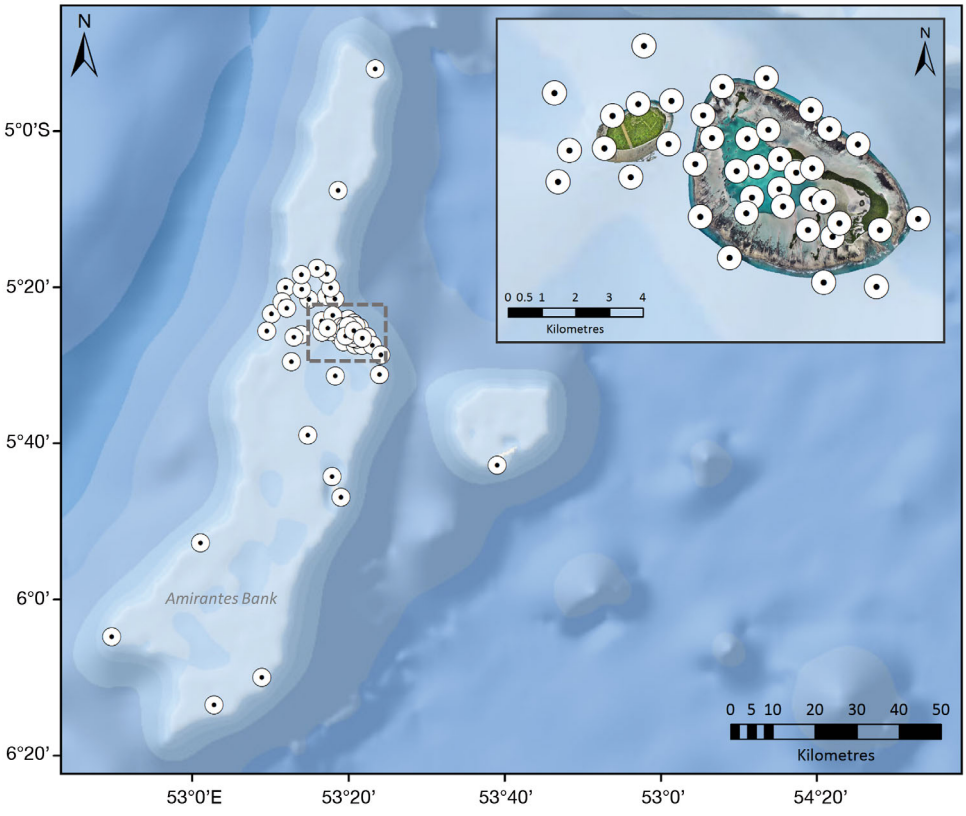

Fig. 2. Distribution of acoustic receivers (n = 70) throughout the Amirante Islands. The box outlines the area shown in the inset, indicating increased receiver density around D'Arros Island and St. Joseph Atoll. Receiver locations marked with ⊙. Maps created in ArcGIS (www.esri.com/) using GEBCO_08 (version 20100927) bathymetry data. Satellite imagery © Save Our Seas Foundation

2.4. Spatio-temporal analyses

The distribution and connectivity of detections throughout the receiver array were visualised and analysed using the packages 'igraph' (Csardi & Nepusz 2006) and 'ggplot2' (Wickham 2016) in R (version 3.4.1; R Core Team 2017), before being presented in ArcMap 10.3® (ESRI). Briefly, each acoustic receiver was considered to be a node within a network, and the size of each node was drawn to represent the number of detections recorded at that receiver. The line thickness of the edges connecting the nodes were then drawn relative to the frequency at which *M. alfredi* travelled between each pair of receivers (Jacoby et al. 2012). The sequential detection of tagged *M. alfredi* throughout the receiver array from the first detection to the last is hereafter referred to as the 'track' for each individual.

The mean distance travelled per day by each individual was calculated by averaging the cumulative distance between detections across receivers within a 24 h period. This metric represents the minimum distance travelled per day for each *M. alfredi*, as the extent of movement of any individual that travelled beyond the detection boundary of the receiver array could not be quantified. A 1-way ANOVA was used to determine whether female and male *M. alfredi* travelled the same mean distance per day, and linear regression was used to examine the potential relationship between wingspan (i.e. maturity status) and distance travelled per day. Data homogeneity and normality were confirmed through Levene's and Shapiro-Wilk tests, respectively.

Broad scale residency was measured using a residency index (RI; Daly et al. 2014) defined as:

$$\mathrm{RI}(\%) = \frac{\text{No. of days detected}}{\text{No. of days between first and last detection}} \quad (1)$$

On 5 occasions, an individual that had shed a tag deployed in Period One was then re-tagged in Period Two. For these mantas, RI values were averaged across both deployments. Residency indices were used to infer the amount of time that tagged *M. alfredi* were spending inshore of the Amirante Islands and at D'Arros Island and St. Joseph Atoll. One- and 2-way ANOVAs were used to determine whether residency indices differed significantly with sex and wingspan (i.e. life stages) of tagged individuals. Assumptions of normality and homogeneity were met in all cases, as verified with Shapiro-Wilk and Levene's tests, respectively.

Differences in patterns of local residency to the Amirantes between the sexes and life stages of *M. alfredi* were further investigated by considering at which receivers, and how frequently, individuals were detected within the array. The number of track days that individuals were detected at each receiver was calculated to examine the extent of array use (A), and the proportion of total detections recorded at each receiver per individual was used as a measure of residency to each site (B; Papastamatiou et al. 2010). Prior to analysis, counts of detection days were $\log(x+1)$ transformed to allow for better comparisons among individuals with differing track lengths, whereas proportion data were transformed to arcsine-square root values (Meyer et al. 2010, Papastamatiou et al. 2010). Bray-Curtis similarity matrices were then constructed (PRIMER-E Version 6), and non-metric multidimensional scaling plots were used to visualise potential differences in A and B among tagged individuals. ANOSIM measures were used to assess whether array use or residency varied significantly between male and female *M. alfredi* of various life stages, and if these patterns were the same between the 2 deployment periods of this study. All ANOSIMs were programmed to process up to 9999 permutations, and significant differences between groups were defined at $p < 0.05$.

2.5. Environmental modelling

Generalised additive mixed models (GAMMs) were used to investigate how temporal, biological and environmental factors may influence the occurrence of *M. alfredi* at D'Arros Island and St. Joseph Atoll. Models considered the presence of *M. alfredi* at receivers within 2.5 km of these locations between November 2016 and September 2017, and this time frame was selected because it provided the greatest availability of environmental data within the overall study period. Nine continuous variables were examined during the modelling process: day of the year, time of day, fraction of moon illuminated, time relative to high tide, tidal range, water temperature, prevailing wind direction, wind speed and wingspan (Table 1). Sex of individual was also included as a categorical factor. All predictors were selected for inclusion because they have been shown to influence the occurrence (Couturier et al. 2018, Setyawan et al. 2018) and behaviour (O'Shea et al. 2010, Jaine et al. 2012) of *M. alfredi* at other locations. Behavioural differences among individuals that may influence the frequency of occurrence at D'Arros Island were accounted for by including manta ray ID as a random effect in all models. Inclusion of this random factor

Table 1. Description of variables used in GAMM analysis of reef manta ray *Mobula alfredi* occurrence at D'Arros Island and St. Joseph Atoll, Seychelles

Variable	Type of effect	Units/levels	Description
Sex	Fixed: categorical fitted with natural spline (k = 5)	Female, male	Sex of tagged individuals
Wingspan	Fixed: continuous,	0.1 m	Wingspan of tagged individuals
Day of year	Fixed: continuous, fitted with harmonic polynomial (k = 5)	1–365	Day of the year
Hour of day	Fixed: continuous, fitted with harmonic polynomial (k = 5)	0–23	Hour of the day
Moon illumination	Fixed: continuous, fitted with natural spline (k = 5)	0.00–1.00	Fraction of moon illuminated by the sun
Time to high tide	Fixed: continuous, fitted with natural spline (k = 5)	1 h	Time relative to most recent or next high tide
Tidal range	Fixed: continuous, fitted with natural spline (k = 5)	0.01 m	Tidal range measured between subsequent high and low tides
Wind speed	Fixed: continuous, fitted with natural spline (k = 5)	0.1 km h^{-1}	Square root of hourly wind speed
Wind direction	Fixed: continuous, fitted with harmonic polynomial (k = 5)	1°	Hourly wind direction
Water temperature	Fixed: continuous, fitted with natural spline (k = 5)	0.1°C	Hourly water temperature at a cleaning station north of D'Arros Island
Manta ID	Random	Individual tag ID	Identifies individual manta rays

also controlled for pseudo-replication arising from the repeated measure of the same individuals throughout the study period (Couturier et al. 2018).

Day of the year and hourly values were extracted from detection data, whereas daily lunar illumination data for Seychelles were obtained from the United States Naval Observatory website (http://aa.usno.navy.mil/data/docs/MoonFraction.php). Both tidal metrics (tidal range and time relative to high tide) were assigned to hourly detection periods based on measures of tidal height as calculated by a tidal model built using the Oregon State University Tidal Model Driver (Egbert & Erofeeva 2002, Lea 2017). Modelled tidal cycles were based on the harmonics for St. Joseph Atoll's location, with the final model predicting tidal heights in metres every 10 min that were subsequently averaged over each hour of the study period. Wind speed and direction data were collected every 30 min by a weather station (Davis 6152 Wireless Vantage Pro2; Davis Instruments) deployed at D'Arros Island. Water temperature data were collected every 10 min by a temperature logger (Onset HOBO Water Temperature Pro-v2) deployed to the north of D'Arros Island at approximately 15 m depth. These records were subsequently averaged over each hour of the study period and aligned with the acoustic detection data.

GAMMs were constructed with a binomial error structure and log link function using maximum likelihood estimations in the package 'mgcv' (Wood 2017). The presence of individual manta rays within the array was quantified as either '1' (present) or '0' (absent) for each hour of the study period based on whether a detection had been recorded for that individual during that time. Harmonic polynomials were fitted to the cyclical factors 'time of day', 'day of year' and 'wind direction' to ensure continuity between records (Jaine et al. 2012), whereas the square root values of wind speed were used to normalise the skewed distribution of data available for that predictor. The function 'cor' in R was used to ensure that there was no strong cross-correlation between continuous predictors (Table S1 in the Supplement at www.int-res.com/articles/suppl/m621p169_supp.pdf).

Significant predictors of *M. alfredi* occurrence at D'Arros Island and St. Joseph Atoll were identified from the complete suite of variables through a full-subset model selection approach using the package 'MuMIn' (Barton & Barton 2016). All potential combinations of predictor variables were considered, and each fitted within a separate GAMM. Akaike's information criterion corrected for sample size (AICc) and AICc weight (wAICc) were then used to select the highest ranking model, with wAICc able to vary be-

tween 0 (no support) and 1 (complete support; Ferreira et al. 2017). Models within 2 AICc units of each other were considered to be equally ranked. When the difference in AICc values (ΔAICc) between top candidate models was <2, the model containing the lowest number of explanatory variables (i.e. the most parsimonious) was selected as the appropriate model for the data.

The contribution of each significant predictor variable to the final GAMM was assessed using likelihood-ratio tests that compared the fit of the final model to a model omitting the respective predictor variable as described by Jaine et al. (2012). Marginal effects for each predictor in the final model were visualised using the 'plot.gam' function ('mgcv'), where the scale on the *y*-axis was relative to the magnitude of the effect, and the shape indicated the direction of influence of that predictor on manta occurrence at D'Arros Island and St. Joseph Atoll (Jaine et al. 2012).

3. RESULTS

3.1. Detection summary

Of the 42 acoustic tags deployed on *Mobula alfredi* for this study, 38 tags returned usable tracks from 33 individuals (Table 2). A total of 164 336 detections were recorded across the study period, with females accounting for 34.6% of detections and males for 65.4% (n = 16 and 17, respectively; Fig. 3). Of the females that were tagged, 1 was juvenile, 4 were sub-adults, and 11 were adults (4.0, 5.9 and 18.5% of total detections, respectively). Of the males that were tagged, 2 were juvenile, 6 were sub-adults, and 9 were adults (41.0, 12.1 and 18.4% of total detections, respectively). Tags remained on individuals for an average of 247 ± 170 d, with a minimum retention time of 19 d and a maximum retention time of 776 d.

3.2. Spatial movements

Individuals moved widely throughout the Amirantes receiver array (Fig. 4), travelling mean distances of 13.3 ± 2.9 km d^{-1} and a maximum of 89.3 km d^{-1}. There were no significant differences in the average daily distances travelled by males and females ($F_{1,36}$ = 0.68, p = 0.41), but daily distance travelled increased with increasing wingspan (i.e. maturity level; $F_{1,36}$ = 3.39, p = 0.07, adj. R^2 = 0.06). Only a single tagged individual with a wingspan <3.0 m was found to travel an average of >20 km d^{-1} (SC-MA-0020; juvenile male). When this individual was removed from the analysis, the relationship between wingspan and average daily distance travelled became even more apparent ($F_{1,35}$ = 6.16, p = 0.02, adj. R^2 = 0.13).

The majority of detections (n = 145 677; 89% of total) of *M. alfredi* were recorded at the receivers located within 2.5 km of D'Arros Island and St. Joseph Atoll (inset, Fig. 4). No detections were recorded inside the St. Joseph Atoll lagoon, and only 4 detections from a single individual (SC-MA-0027; mature female) were recorded at the easternmost Desroches receiver. *M. alfredi* were most frequently detected on the northern side of D'Arros Island in proximity to a site where *M. alfredi* were observed to visit and clean consistently (hereafter, 'cleaning station'; Potts 1973; $n_{detections}$ = 48 766; 29.7% of total; Fig. 4). A large amount of activity was also recorded in the channel between D'Arros Island and St. Joseph Atoll, where *M. alfredi* are often seen feeding at the surface.

3.3. Residency in the Amirantes

3.3.1. Broad scale (10–100 km)

On average, tagged *M. alfredi* were detected throughout the Amirantes on 62% of the days that they were tracked (RI = 61.9 ± 23.0%), with a minimum RI of 11.1% and maximum RI of 97.1% (Table 2). A 2-way ANOVA suggested that there was no difference in RI according to sex ($F_{1,31}$ = 1.81, p = 0.188), but that RI decreased significantly with increasing wingspan (i.e. maturity level; $F_{1,31}$ = 13.58, p < 0.001). Juvenile *M. alfredi* were observed to spend a greater amount of time (RI = 76.0 ± 14.2%) within range of the receiver array than adults (RI = 45.6 ± 23.8%), regardless of their sex ($F_{3,29}$ = 4.77, $p_{wingspan \times sex}$ = 0.52).

Multivariate analyses indicated that when tagged *M. alfredi* were present within the Amirantes receiver array, there was no significant difference in the frequency at which either sex, or any of the maturity groups, visited the different receivers (R = –0.02, p = 0.77, and R = –0.02 and p = 0.35, respectively), or in the amount of time spent in proximity to the receivers (R = 0.01, p = 0.35 and R = –0.04, p = 0.67, respectively; Fig. S1). Additionally, there were no differences in receiver visitation patterns, or time spent in proximity to receivers, between the 2 deployment periods (R = 0.05, p = 0.09 for both metrics; Fig. S1).

Table 2. Summary of acoustic tag deployments on reef manta rays *Mobula alfredi* at D'Arros Island, Seychelles, from November 2013 to October 2017. Dates are given as d/mo/yr. Det.: detections; Av. Dist.: average distance travelled; DSTJ: D'Arros Island and St. Joseph Atoll

Manta ID	Sex	Size (m)	Tag ID (tag type)	Deployment date	Last detection	Total no. det	Total track days	Total det. days	Residency index (%)	Av. Dist. (km d^{-1})	Tracking days at DSTJ (%)	Detection days at DSTJ (%)
SC-MA-0001	M	2.8	28222 (V16-5H)	30/11/2013	15/04/2014	5681	137	133	97.1	14.7	91.2	94.0
SC-MA-0002	M	3	28248 (V16-5H)	15/11/2016	23/10/2017	7070	343	204	59.5	12.1	51.3	86.3
SC-MA-0005	M	2.7	28240 (V16-5H)	17/12/2013	31/01/2016	30504	776	685	88.3	15.7	72.3	81.9
SC-MA-0006	M	3	28245 (V16-5H)	15/11/2016	30/04/2017	1554	167	97	58.1	13.1	28.7	49.5
SC-MA-0011	F	3.8	28227 (V16-5H)	08/12/2013	30/05/2014	5589	174	151	86.8	12.7	78.7	90.7
SC-MA-0012	F	3.5	28239 (V16-5H)	16/12/2013	04/08/2014	4451	232	162	69.8	9.6	55.2	79.0
SC-MA-0014	F	3.1	28242 (V16-5H)	18/12/2013	07/03/2015	20655	445	395	88.8	12.7	76.2	85.8
SC-MA-0016	M	3.1	28224 (V16-5H) & 27120 (V16-5H)	06/12/2013 & 13/11/2016	28/02/2015 & 13/01/2017	11289	512	334	65.2	12.2	36.3	55.7
SC-MA-0017	F	3.5	15038 (V16TP-5H)	22/11/2016	04/03/2017	1016	103	83	80.6	13.5	68.9	85.5
SC-MA-0019	M	2.5	28229 (V16-5H)	12/12/2013	17/11/2014	14198	341	305	89.4	12.7	68.6	76.7
SC-MA-0020	M	2.8	28228 (V16-5H) & 28246 (V16-5H)	11/12/2013 & 17/11/2016	17/05/2017 & 27/12/2016	6559	199	162	81.4	17.7	71.9	88.3
SC-MA-0021	F	3.1	27121 (V16-5H)	14/11/2016	22/03/2017	2229	129	90	69.8	9.6	64.3	92.2
SC-MA-0025	F	3.6	15042 (V16TP-5H)	25/11/2016	20/01/2017	425	57	34	59.6	19.7	38.6	64.7
SC-MA-0026	M	3.2	28244 (V16-5H)	14/11/2016	02/12/2016	161	19	8	42.1	9.3	26.3	62.5
SC-MA-0027	F	3.7	27118 (V16-5H)	15/11/2016	23/10/2017	353	343	38	11.1	19.4	1.7	15.8
SC-MA-0031	M	2.4	28220 (V16-5H)	16/11/2013	13/04/2014	2344	149	98	65.8	13.6	12.1	18.4
SC-MA-0044	M	3	27117 (V16-5H)	11/11/2016	20/05/2017	3288	191	150	78.5	10.7	70.2	89.3
SC-MA-0052	M	2.6	28241 (V16-5H) & 28236 (V16-5H)	18/12/2013 & 14/11/2016	15/04/2014 & 21/06/2017	8683	339	265	78.2	13.0	72.3	92.5
SC-MA-0053	M	2.9	15044 (V16TP-5H)	25/11/2016	16/10/2017	1297	326	138	42.3	12.9	36.5	86.2
SC-MA-0073	M	3.3	28234 (V16-5H)	15/03/2014	06/10/2014	1575	206	116	56.3	11.3	20.4	36.2
SC-MA-0075	M	2.9	28231 (V16-5H)	15/12/2013	10/10/2014	3409	300	150	50.0	13.4	24.0	48.0
SC-MA-0077	F	3.6	28226 (V16-5H)	08/12/2013	23/04/2014	1232	228	66	28.9	14.6	14.5	50.0
SC-MA-0078	F	3.8	15036 (V16TP-5H)	18/11/2016	12/10/2017	747	329	99	30.1	15.0	15.8	52.5
SC-MA-0079	F	3.7	28223 (V16-5H)	06/12/2013	22/03/2014	963	107	49	45.8	12.4	2.8	6.1
SC-MA-0084	F	2.4	28221 (V16-5H) & 15040 (V16TP-5H)	30/11/2013 & 24/11/2016	19/01/2014 & 25/10/2017	6581	387	339	87.6	10.7	82.2	93.8
SC-MA-0087	M	2.6	28232 (V16-5H)	16/12/2013	23/07/2014	1836	220	116	52.7	14.1	17.7	33.6
SC-MA-0094	M	3	28238 (V16-5H)	14/11/2016	17/02/2017	607	96	60	62.5	10.9	17.7	28.3
SC-MA-0101	F	3.5	28237 (V16-5H)	14/11/2016	14/07/2017	915	243	89	36.6	18.2	11.1	30.3
SC-MA-0107	F	3	15050 (V16TP-5H)	26/11/2016	20/10/2017	3579	329	266	80.9	12.3	72.3	89.5
SC-MA-0110	F	2.6	15048 (V16TP-5H)	26/11/2016	25/10/2017	3960	334	274	82.0	11.8	76.9	93.8
SC-MA-0115	M	2.7	27119 (V16-5H)	11/11/2016	25/10/2017	7401	349	253	72.5	8.5	69.6	96.0
SC-MA-0128	F	3.5	28235 (V16-5H) & 15046 (V16TP-5H)	22/03/2014 & 26/11/2016	24/04/2016 & 07/05/2017	3856	928	269	29.0	13.9	7.2	24.9
SC-MA-0134	F	3.7	15034 (V16TP-5H)	18/11/2016	18/10/2017	329	335	52	15.5	16.3	7.2	46.2
					Average	4979.9	284.0	173.6	61.9	13.3	44.3	64.4

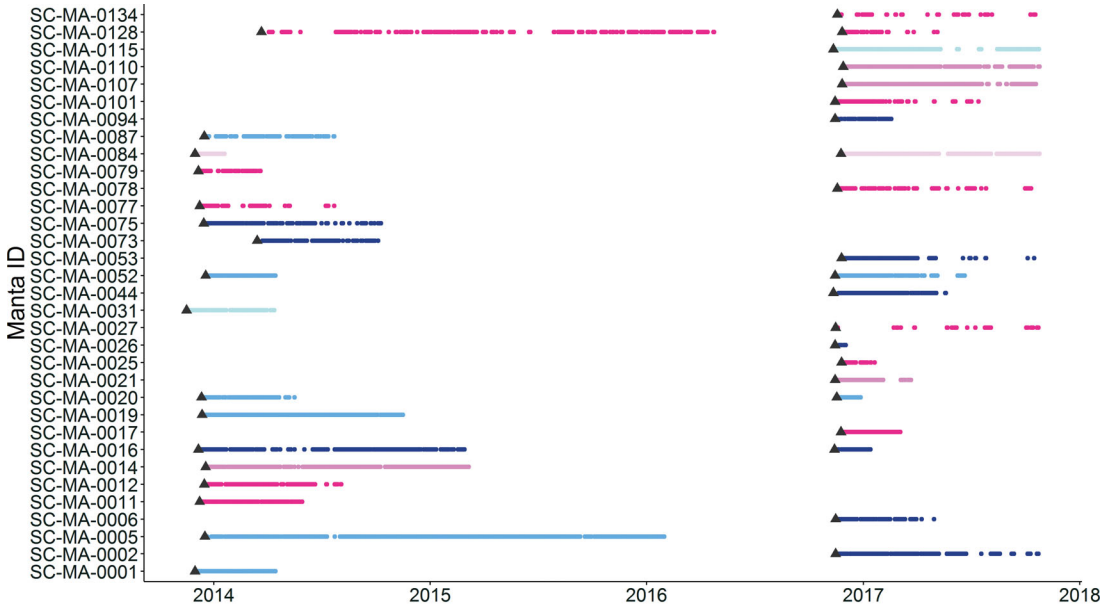

Fig. 3. Summary of reef manta ray *Mobula alfredi* detections recorded across the Amirantes receiver array between November 2013 and October 2017 for tracks lasting longer than 7 d. Colours show sex (blues: male; reds: female) and life stage (lightest colour shades: juvenile; intermediate shades: sub-adult; dark shades: adult) of each individual. Tag deployment dates are indicated by triangles

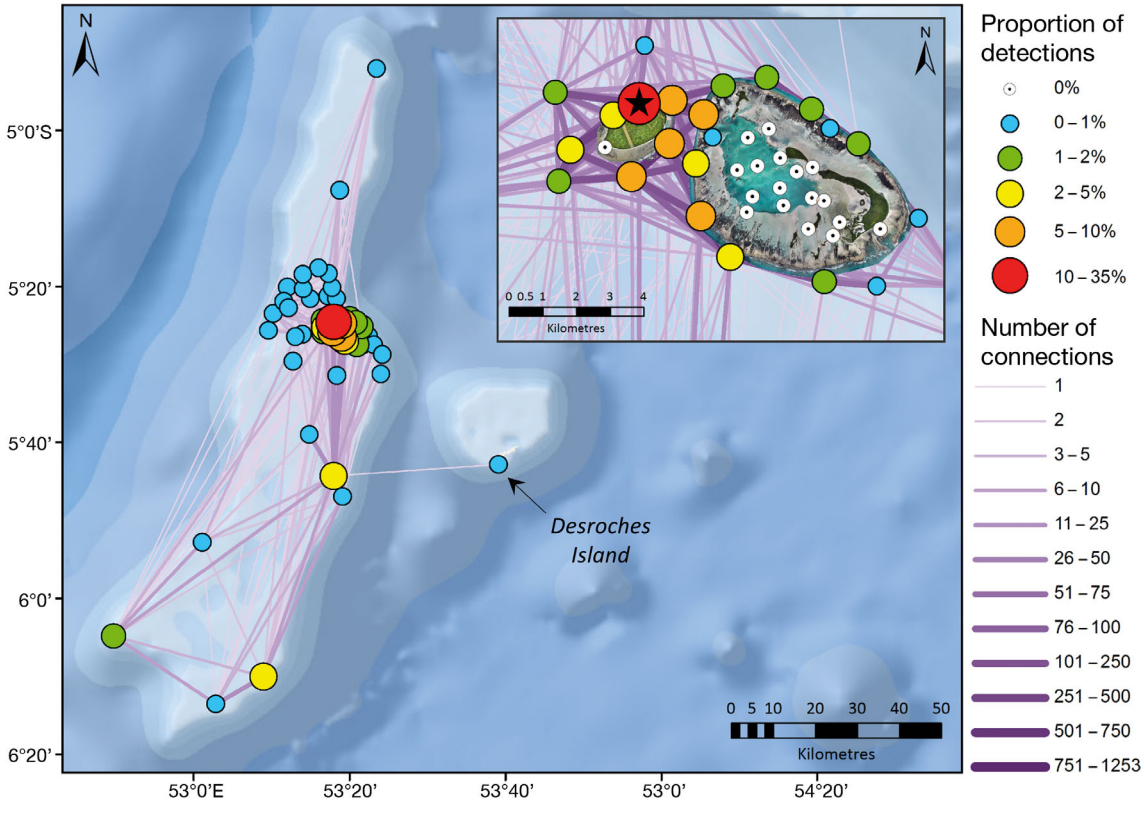

Fig. 4. Network map of the Amirantes receiver array, indicating the proportion of reef manta ray *Mobula alfredi* detections recorded at each receiver (nodes; n = 70) between November 2013 and October 2017. Edges represent the frequency of subsequent detections between receivers. Symbology is described in the legend. Cleaning station location indicated by the star. Maps created in ArcGIS 10.3 (www.esri.com/) using GEBCO_08 (version 20100927) bathymetry data. Satellite imagery © Save Our Seas Foundation

3.3.2. Local scale (1–10 km)

Individual *M. alfredi* appeared to be largely resident at D'Arros Island and the neighbouring St. Joseph Atoll. On average, individuals were recorded at the receivers positioned within 2.5 km of these islands on 47.6 ± 30.6% of all of the days that they were tracked and on 66.7 ± 28.0% of all days that they were detected within the entirety of the Amirantes array (Table 2). During the first deployment period, a juvenile female (SC-MA-0084) was recorded only at the inshore receivers around D'Arros Island and St. Joseph Atoll for the 51 d that she was tracked. Of the other 32 individuals that were tagged across both deployment periods and were observed to have left this area, all except 1 (SC-MA-0079, mature female) returned to D'Arros Island and St. Joseph Atoll on at least 1 occasion while being tracked (Fig. S2).

3.4. Temporal and environmental patterns

The final GAMM developed through the model selection process considered 77 414 observations of *M. alfredi* presence and absence at D'Arros Island and St. Joseph Atoll and described 15.0% of the variation present in these data (wAIC = 0.22; Table S2). All temporal and environmental predictors considered during the model selection process were included in the final model, whereas the biological predictors (sex and wingspan) were excluded (Table 3).

Table 3. Summary of the GAMM constructed to assess the influence of temporal, biological and environmental variables on the occurrence of reef manta rays *Mobula alfredi* at D'Arros Island and St. Joseph Atoll, Seychelles. Values are provided for predictors included in the final selected GAMM only. % DE: percent of deviance explained; (–): biological predictors that were excluded from the final model. NA: not applicable

Predictor added to model	Deviance	df	p (χ^2)	% DE
Sex	–	–	–	–
Wingspan (m)	–	–	–	–
Day of year	330.42	2.54	<0.001	0.68
Time of day (h)	1599.40	2.32	<0.001	3.30
Fraction of moon illuminated	46.10	5.57	<0.001	0.10
Time to high tide (h)	20.72	3.57	<0.001	0.04
Tidal range (m)	71.32	4.61	<0.001	0.15
Water temperature (°C)	57.33	4.30	<0.001	0.12
Wind direction (°)	18.23	2.05	<0.001	0.04
Wind speed (km h^{-1})	6.18	2.17	0.05	0.01
Manta ID	4955.40	18.98	<0.001	10.24
Full model	48409.44	7772.01	NA	15.00

The probability of *M. alfredi* being detected within 2.5 km of D'Arros Island and St. Joseph Atoll peaked between November and April (Fig. 5A), coinciding with arrival and departure of the north-west monsoon and the prevailing wind (Fig. 5B) that occurs during these months in Seychelles. Individuals were more likely to be detected during the day (06:00–18:00 h) than at night (18:00–06:00 h; Fig. 5C). Water temperature ranged from 25.3 to 30.6°C during the study period. Detection frequencies for *M. alfredi* peaked when the water temperature was approximately 28°C (Fig. 5D). Additionally, individuals were more likely to be detected during a new moon (Fig. 5E), when the tidal range was at its highest (Fig. 5F), and on the slack of high tide (Fig. 5G). Individuals were less likely to be detected at this location as wind speed increased (Fig. 5H). Finally, differences in visitation patterns among individuals explained the largest amount of variation in these data (10.2%; Table 3).

4. DISCUSSION

4.1. Spatial movements through the Amirantes

Tagged *Mobula alfredi* were resident in the area of D'Arros Island and St. Joseph Atoll, spending an average of 64.4% of the tracking days within 2.5 km of these locations. Movements of individuals along the length of the Amirantes Bank (152 km) were infrequent and tended to favour the eastern ridge of the Bank. Although reef manta rays have a circumtropical distribution (Couturier et al. 2012), such patterns of high residency and relatively restricted movements away from aggregation sites appear to be typical of most localities (Jaine et al. 2014, Couturier et al. 2018, Stewart et al. 2018a). Broad-scale movements do occur, for example in the waters of eastern Australia, where *M. alfredi* travelled across a range of up to 1035 km (Jaine et al. 2014); however, movements of individuals are typically limited to <500 km (Couturier et al. 2011, Germanov & Marshall 2014, Braun et al. 2015, Setyawan et al. 2018).

Only 1 *M. alfredi* was detected at Desroches Island (50 km from D'Arros Island; position shown in Fig. 4) during our 4 yr study. This individual (SC-MA-0027; mature female) travelled 40 km across waters up to 1500 m in depth from northern Poivre (17 November 2016) to Desroches Island (19 November 2016), where 2 detections were recorded over a period of 2 min. The same individual briefly returned to Desroches Island on 21 February 2017 when another

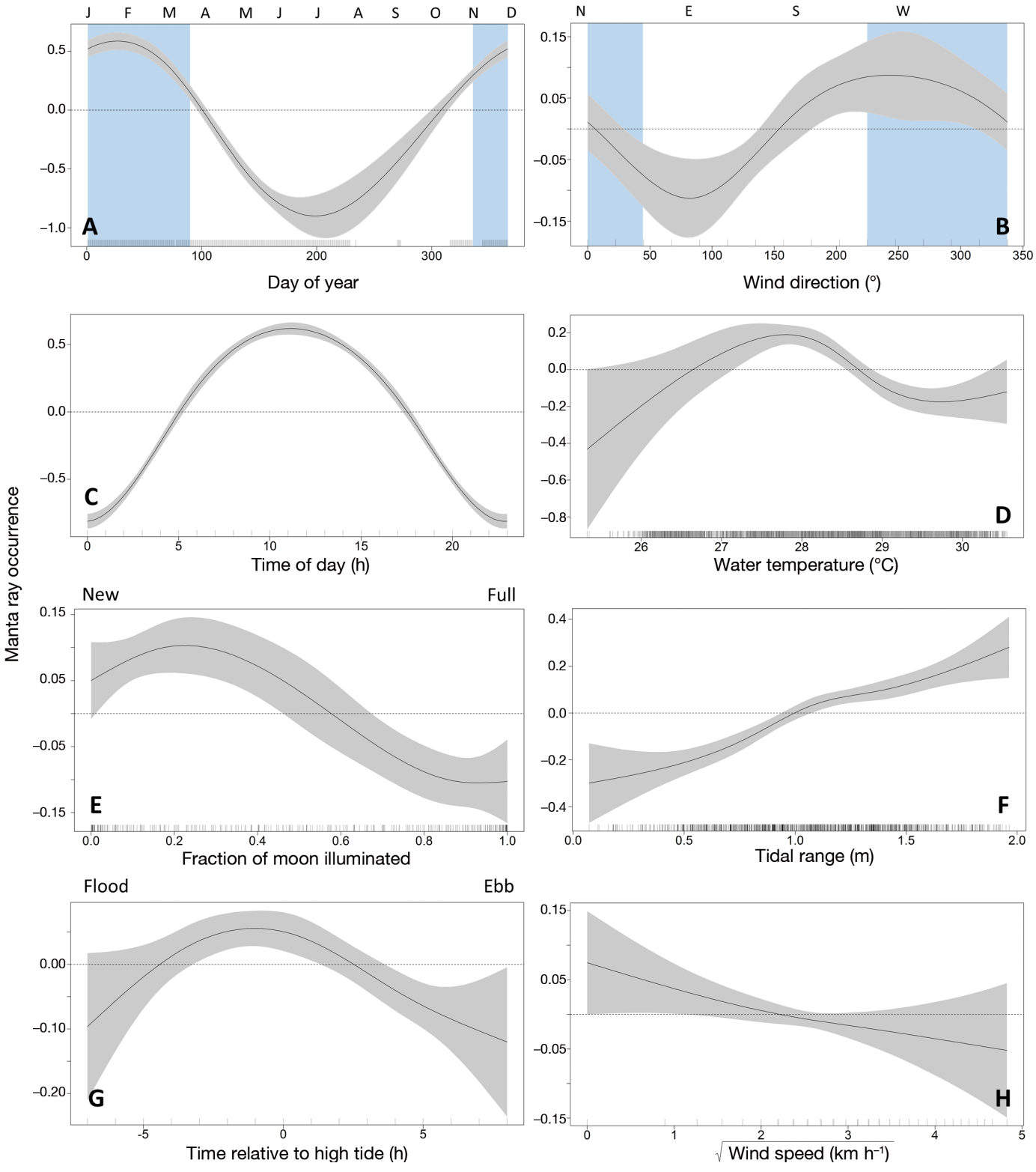

Fig. 5. Marginal effect plots derived from the top ranked binomial GAMM indicating the significant effects of (A) day of year (letters at the top represent months of the year), (B) prevailing wind direction (letters at the top represent cardinal directions), (C) time of day, (D) water temperature, (E) fraction of moon illuminated, (F) tidal range, (G) time relative to high tide and (H) wind speed on the probability of detecting acoustically tagged reef manta rays *Mobula alfredi* at D'Arros Island and St. Joseph Atoll between November 2016 and September 2017. Blue shading indicates periods of north-west monsoon. Grey shading indicates 95% confidence interval. Horizontal dashed lines indicate $y = 0$

2 detections were recorded, and was detected again on the main Amirantes Bank 6 d later. This was the first confirmed movement of *M. alfredi* between D'Arros Island and Desroches Island, and only 1 additional movement has been recorded since using photo-identification (L. Peel unpubl. data). Evidence from Japan and Indonesia suggests that *M. alfredi* are easily capable of inter-island movements at this spatial scale (350–450 km; Homma et al. 1999, Germanov & Marshall 2014); however, such movements of individuals between the Amirante Islands appear to be infrequent.

The small number of detections of *M. alfredi* recorded at Desroches Island could be the result of the single receiver at this location being placed in an area that was not suitable habitat for *M. alfredi*, and so failing to record their presence. Alternatively, the channel (up to 1500 m deep) between the main Amirantes Bank and Desroches Island may act as a barrier to movement, possibly because it places individuals at greater risk of predation (Marshall & Bennett 2010, Deakos et al. 2011). It is also possible that sufficient food resources may exist on the Amirantes Bank, so that it is unnecessary for individuals to travel elsewhere (Deakos et al. 2011). A lack of cross-channel movements of *M. alfredi* has similarly been noted in Hawaii, where none of the 435 individually identified mantas were found to have traversed the 47 km wide and 2000 m deep channel between Maui and the Big Island during a 10 yr study (Deakos et al. 2011). Our study provides further support to the possibility that deep water may act as a barrier to the movements of this species.

4.2. Residency and array use

Tagged individuals showed high levels of residency to the Amirante Islands (mean RI = 61.9%), with a maximum residency index of 97.1% recorded over 137 tracking days (SC-MA-0001; sub-adult male). Similar levels of residency have been reported for *M. alfredi* using passive acoustic telemetry in the Red Sea (RI = 65.1%; Braun et al. 2015), but the RIs recorded in our study are much higher than those recorded from arrays in eastern Australia (15%; Couturier et al. 2018) and Hawaii (39.1%; Clark 2010). These latter studies also included receivers that were placed at known cleaning stations, but deployed fewer receivers compared to the Amirante array (6 and 43, respectively), which may have contributed to a lower likelihood of detection and thus apparent residency.

Juvenile *M. alfredi* displayed greater residency at the Amirantes Bank than adults. A variety of factors might contribute to this pattern, including the possibility that juveniles face an increased threat of predation when travelling away from the refuge of the reef flats of D'Arros Island and St. Joseph Atoll (Heupel et al. 2007, 2018, Cerutti-Pereyra et al. 2014, Stewart et al. 2018b). Juveniles may also lack experience in locating foraging opportunities offshore, and due to smaller body mass may have limited abilities to forage in these deeper, cooler waters (Ware 1978, Sims et al. 2006). Alternatively, or in addition, the lower swimming efficiency of juvenile *M. alfredi* due to their smaller size might also restrict movement behaviour in comparison to the larger adults (Weihs 1973, Nøttestad et al. 1999).

Movement patterns between, and duration of visitation events to, the islands of the Amirantes region did not differ between the sexes and life stages of *M. alfredi*. D'Arros Island and St. Joseph Atoll, in particular the channel between them and the northern coast of D'Arros Island, were key locations for all tagged individuals. The high use of this restricted area by all individuals in this study suggests that the establishment of an MPA covering D'Arros Island and St. Joseph Atoll would provide conservation and management benefits for *M. alfredi*.

4.3. Environmental and temporal patterns

The occurrence of tagged *M. alfredi* varied with the shifting trade winds of the annual monsoons, with a steep decline in detection probability from March to July when the north-western monsoon began to subside, and higher detection frequencies occurring during southern winds. Given that the trade winds play a critical role in the development of surface currents and subsequently how plankton accumulates in the water column (Gove et al. 2016), it is possible that these changing wind regimes alter zooplankton accumulation at D'Arros Island and St. Joseph Atoll as it does across the islands of the Maldives (Anderson et al. 2011). The resulting fluctuation in food availability for *M. alfredi* may drive the subsequent changes of presence of individuals at this location.

Tidal phase also had a significant influence on the presence of *M. alfredi* at D'Arros Island and St. Joseph Atoll. Occurrence was highest in the hours before and during a high tide, and when the tidal range was at a maximum (approximately 2 m). These trends in detections were additionally supported by sighting and photo-identification records collected at

D'Arros Island (L. R. Peel unpubl. data). Tides also influenced the cleaning and foraging behaviours of *M. alfredi* on the Great Barrier Reef (O'Shea et al. 2010, Jaine et al. 2012, Couturier et al. 2018), where cleaning behaviour was most commonly observed at, and after, a high tide, and foraging behaviour on large, ebbing tides (Jaine et al. 2012). As our receivers were located close to a cleaning station and in the St. Joseph Channel, where feeding behaviour is commonly observed, similar behaviours could account for the increase in detections around high tide at D'Arros Island and St. Joseph Atoll. A slack tide may also increase the frequency of tag detection by reducing the amount of ambient noise present in the surrounding environment through diminished current speeds (Mathies et al. 2014). However, this should occur on both the high and low tides, thus is unlikely to account for our results.

Increasing wind speeds were associated with a reduction in the occurrence of *M. alfredi* around D'Arros Island and St. Joseph Atoll. Similar patterns during high winds have been recorded on the Great Barrier Reef (Jaine et al. 2012, Couturier et al. 2018), with decreased prey concentration, reduced visibility, and increased predation risk being suggested as potential reasons for *M. alfredi* to avoid rough conditions at the surface (Couturier et al. 2018). Additionally, it is possible that these rough sea conditions caused a reduction of receiver efficiency and contributed to the observed pattern of occurrence at D'Arros Island and St. Joseph Atoll (Cagua 2012). The consistency of response by *M. alfredi* to increasing wind speeds at various study sites, however, suggests that this is a component of their behaviour rather than an artefact of ambient noise (Jaine et al. 2012, Couturier et al. 2018).

Detection frequencies of *M. alfredi* at D'Arros Island and St. Joseph atoll were greater during the day than at night. This pattern suggests that individuals move beyond the boundary of the receiver array at night, potentially travelling offshore and beyond the Amirantes Bank where the majority of the receivers were located. This finding also supports the idea that *M. alfredi* vary their foraging strategy throughout the diel cycle. Individuals are thought to feed at the surface of shallow reef flats during the day, before venturing into deeper waters during the night, where they forage on emergent and benthic zooplankton communities (Couturier et al. 2013, Burgess et al. 2016). This behavioural pattern has been recorded in numerous localities, including Indonesia (Dewar et al. 2008, Setyawan et al. 2018), Hawaii (Clark 2010, Deakos et al. 2011), the Red Sea (Braun et al. 2014) and eastern Australia (Couturier et al. 2018). Alternatively, or in addition, higher detection frequencies during the day may also be driven by the physiological needs of individuals. Occupation of the shallow waters of the reef flats during the day might allow *M. alfredi* to warm their regionally endothermic bodies (Alexander 1996, Thorrold et al. 2014) to favourable temperatures prior to undertaking deep or offshore feeding behaviours at night (Braun et al. 2014).

The strong diel cycle observed in the inshore visitation pattern of *M. alfredi* might also be explained by their use of cleaning stations during daylight hours. Visitation frequencies of *M. alfredi* to cleaning stations elsewhere have tended to occur from late morning to early afternoon (Dewar et al. 2008, Clark 2010, O'Shea et al. 2010, Jaine et al. 2012, Couturier et al. 2018, Setyawan et al. 2018), since cleaner fishes are only active and therefore available for parasite removal during the daytime (Potts 1973, Lenke 1988, Côté 2000, Marshall & Bennett 2010, Couturier et al. 2018). Manta cleaning stations are also believed to facilitate important social interactions among individuals (O'Shea et al. 2010, Deakos et al. 2011, Marshall et al. 2011, Stevens et al. 2018). Attendance at the cleaning station at D'Arros Island for either of these reasons would have brought tagged *M. alfredi* close to receiver stations during the day, increasing the likelihood of tag detections. Additionally, we acknowledge that a reduced receiver detection range resulting from increased levels of biological noise on the coral reef at night may have contributed to the observed patterns of detection (Cagua 2012, How & de Lestang 2012).

Finally, there was a higher frequency of detections of *M. alfredi* during the new moon than the full moon at D'Arros Island and St. Joseph Atoll. This pattern appears common to the species, with lower frequencies of detection of tagged individuals occurring during the full moon in receiver arrays on the Great Barrier Reef (Couturier et al. 2018) and, in the Red Sea, satellite-tagged *M. alfredi* diving deeper during a full moon than a new moon in offshore waters (Braun et al. 2014). Similar patterns of movement have been recorded in other elasmobranchs in coral reef environments (Vianna et al. 2013, Hammerschlag et al. 2017) and are thought to reflect changes in the distribution of prey, or risk of predation to individuals with increased light in the upper water column (Hays 2003, Hammerschlag et al. 2017). For *M. alfredi*, a full moon may limit the extent of movement of zooplankton prey to shallow water at night. This would require tagged individuals to travel into deeper, off-

shore waters to forage, causing individuals to exit the boundary of the receiver array and decrease their likelihood of detection. Conversely, during a new moon, zooplankton may rise close to the surface, allowing *M. alfredi* to forage on this prey close to D'Arros Island and St. Joseph Atoll on the shallow Amirantes Bank. This behavioural pattern would bring tagged individuals within range of the receivers at this location during a new moon, and increase their likelihood of detection during this time.

5. SUMMARY

The patterns of high residency and similarity of movements of all components of the population suggest that the establishment of an MPA at D'Arros Island and St. Joseph Atoll would be a beneficial conservation and management strategy for *Mobula alfredi* in the Amirante Islands. This is particularly true for juveniles, which displayed the highest levels of residency at this location regardless of their sex. In addition to protecting *M. alfredi* from targeted fishing pressures, accidental entanglement and boat strikes at D'Arros Island and St. Joseph Atoll, such an MPA would also serve to protect the cleaning station to the north of D'Arros Island and the surrounding coral reef ecosystem. Satellite telemetry and photo-identification data will assist in expanding our current understanding of the movement patterns of this species in the future by providing insight into the broader movements of *M. alfredi* throughout Seychelles as a whole. To date, few confirmed sightings of *M. alfredi* have been recorded outside of the Amirante Islands and the neighbouring Alphonse Islands in Seychelles (<2% of all records, L. R. Peel unpubl. data), despite considerable effort to collect data in these locations. This observation further supports the hypothesis that the Amirante Islands, in particular D'Arros Island and St. Joseph Atoll, are key areas for this Vulnerable species (Marshall et al. 2018). Continued monitoring of *M. alfredi* movement throughout Seychelles will ensure that this species is protected at appropriate scales across this remote area of the western Indian Ocean.

Acknowledgements. All research was approved by, and conducted with the knowledge of, the Seychelles Bureau of Standards, the Seychelles Ministry of Environment, Energy and Climate Change and The University of Western Australia (RA/3/100/1480). This study was funded by the Save Our Seas Foundation (SOSF) and supported by The Manta Trust, The University of Western Australia and the Australian Institute of Marine Science. Field work was supported by the SOSF – D'Arros Research Centre (SOSF-DRC). We thank the editor and 3 anonymous reviewers for their valuable feedback on this manuscript. L.P. thanks L. Ferreira for comments on the data analyses used in this study.

LITERATURE CITED

Alexander RL (1996) Evidence of brain warming in the mobulid rays, *Mobula tarapacana* and *Manta birostris* (Chondrichthyes: Elasmobranchii: Batoidea: Myliobatiformes). Zool J Linn Soc 118:151–164

Anderson RC, Adam MS, Goes JI (2011) From monsoons to mantas: seasonal distribution of *Manta alfredi* in the Maldives. Fish Oceanogr 20:104–113

Barton K, Barton MK (2016) Package 'MuMIn': multi-model inference. R package, version 1.15.6. https://CRAN.R-project.org/package=MuMIn

Braun CD, Skomal GB, Thorrold SR, Berumen ML (2014) Diving behavior of the reef manta ray links coral reefs with adjacent deep pelagic habitats. PLOS ONE 9:e88170

Braun CD, Skomal GB, Thorrold SR, Berumen ML (2015) Movements of the reef manta ray (*Manta alfredi*) in the Red Sea using satellite and acoustic telemetry. Mar Biol 162:2351–2362

Burgess KB, Couturier LI, Marshall AD, Richardson AJ, Weeks SJ, Bennett MB (2016) *Manta birostris*, predator of the deep? Insight into the diet of the giant manta ray through stable isotope analysis. R Soc Open Sci 3:160717

Cagua EF (2012) Factors affecting detection probability of acoustic tags in coral reefs. MSc thesis, King Abdullah University of Science and Technology, Thuwal

Cerutti-Pereyra F, Thums M, Austin CM, Bradshaw CJA and others (2014) Restricted movements of juvenile rays in the lagoon of Ningaloo Reef, Western Australia — evidence for the existence of a nursery. Environ Biol Fishes 97:371–383

Clark TB (2010) Abundance, home range, and movement patterns of manta rays (*Manta alfredi, M. bistrosis*) in Hawai'i. PhD dissertation, University of Hawai'i, Mānoa, HI

Côté IM (2000) Evolution and ecology of cleaning symbioses in the sea. Oceanogr Mar Biol Annu Rev 38:311–355

Couturier LIE, Jaine FRA, Townsend KA, Weeks SJ, Richardson AJ, Bennett MB (2011) Distribution, site affinity and regional movements of the manta ray, *Manta alfredi* (Krefft, 1868), along the east coast of Australia. Mar Freshw Res 62:628–637

Couturier LIE, Marshall A, Jaine F, Kashiwagi T and others (2012) Biology, ecology and conservation of the Mobulidae. J Fish Biol 80:1075–1119

Couturier LIE, Rohner CA, Richardson AJ, Marshall AD and others (2013) Stable isotope and signature fatty acid analyses suggest reef manta rays feed on demersal zooplankton. PLOS ONE 8:e77152

Couturier LIE, Dudgeon CL, Pollock KH, Jaine FRA and others (2014) Population dynamics of the reef manta ray *Manta alfredi* in eastern Australia. Coral Reefs 33:329–342

Couturier LIE, Newman P, Jaine F, Bennett MB and others (2018) Variation in occupancy and habitat use of *Mobula alfredi* at a major aggregation site. Mar Ecol Prog Ser 599:125–145

Csardi G, Nepusz T (2006) The igraph software package for complex network research. InterJ Complex Syst 1695: 1–9

Daly R, Smale MJ, Cowley PD, Froneman PW (2014) Residency patterns and migration dynamics of adult bull sharks (*Carcharhinus leucas*) on the east coast of southern Africa. PLOS ONE 9:e109357

Deakos MH (2012) The reproductive ecology of resident manta rays (*Manta alfredi*) off Maui, Hawaii, with an emphasis on body size. Environ Biol Fishes 94:443–456

Deakos MH, Baker JD, Bejder L (2011) Characteristics of a manta ray *Manta alfredi* population off Maui, Hawaii, and implications for management. Mar Ecol Prog Ser 429:245–260

Dent F, Clarke S (2015) State of the global market for shark products. Fish Aquacult Tech Pap 590. FAO, Rome

Dewar H, Mous P, Domeier M, Muljadi A, Pet J, Whitty J (2008) Movements and site fidelity of the giant manta ray, *Manta birostris*, in the Komodo Marine Park, Indonesia. Mar Biol 155:121–133

Dulvy NK, Fowler SL, Musick JA, Cavanagh RD and others (2014) Extinction risk and conservation of the world's sharks and rays. eLife 3:e00590

Egbert GD, Erofeeva SY (2002) Efficient inverse modeling of barotropic ocean tides. J Atmos Ocean Technol 19: 183–204

Ferreira LC, Thums M, Heithaus MR, Barnett A and others (2017) The trophic role of a large marine predator, the tiger shark *Galeocerdo cuvier*. Sci Rep 7:7641

Germanov ES, Marshall AD (2014) Running the gauntlet: regional movement patterns of *Manta alfredi* through a complex of parks and fisheries. PLOS ONE 9:e110071

Gove JM, McManus MA, Neuheimer AB, Polovina JJ and others (2016) Near-island biological hotspots in barren ocean basins. Nat Commun 7:10581

Graham RT, Witt MJ, Castellanos DW, Remolina F, Maxwell S, Godley BJ, Hawkes LA (2012) Satellite tracking of manta rays highlights challenges to their conservation. PLOS ONE 7:e36834

Hammerschlag N, Skubel RA, Calich H, Nelson ER and others (2017) Nocturnal and crepuscular behavior in elasmobranchs: a review of movement, habitat use, foraging, and reproduction in the dark. Bull Mar Sci 93:355–374

Hamylton S, Spencer T, Hagan AB (2012) Coral reefs and reef islands of the Amirantes Archipelago, Western Indian Ocean. In: Harris PT, Baker EK (eds) Seafloor geomorphology as benthic habitat: GeoHAB atlas of seafloor geomorphic features and benthic habitats. Elsevier, London, p 341–348

Hays GC (2003) A review of the adaptive significance and ecosystem consequences of zooplankton diel vertical migrations. Hydrobiologia 503:163–170

Heinrichs S, O'Malley M, Medd H, Hilton P (2011) Manta ray of hope 2011 Report. The global threat to manta and mobula rays. Manta Ray of Hope Project. www.sharksavers.org/files/9013/3184/4869/The_Global_Threat_to_Manta_and_Mobula_Rays.pdf

Heupel MR, Carlson JK, Simpfendorfer CA (2007) Shark nursery areas: concepts, definition, characterization and assumptions. Mar Ecol Prog Ser 337:287–297

Heupel MR, Kanno S, Martins APB, Simpfendorfer CA (2018) Advances in understanding the roles and benefits of nursery areas for elasmobranch populations. Mar Freshw Res 70:897–907

Holden M (1974) Problems in the rational exploitation of elasmobranch populations and some suggested solutions. In: Harden-Jones FR (ed) Sea fisheries research. Paul Elek, London, p 117–137

Homma K, Maruyama T, Itoh T, Ishihara H, Uchida S (1999) Biology of the manta ray, *Manta birostris* Walbaum, in the Indo-Pacific. In: Seret B, Sire JY (eds) Indo-Pacific fish biology. Proceedings of the 5th Indo-Pacific Fisheries Conference, Noumea, 1997. Ichthyological Society of France, Paris, p 209–216

How JR, de Lestang S (2012) Acoustic tracking: issues affecting design, analysis and interpretation of data from movement studies. Mar Freshw Res 63:312–324

Hussey NE, Kessel ST, Aarestrup K, Cooke SJ and others (2015) Aquatic animal telemetry: a panoramic window into the underwater world. Science 348:1255642

Jacoby DM, Brooks EJ, Croft DP, Sims DW (2012) Developing a deeper understanding of animal movements and spatial dynamics through novel application of network analyses. Methods Ecol Evol 3:574–583

Jaine FRA, Couturier LIE, Weeks SJ, Townsend KA, Bennett MB, Fiora K, Richardson AJ (2012) When giants turn up: sighting trends, environmental influences and habitat use of the manta ray *Manta alfredi* at a coral reef. PLOS ONE 7:e46170

Jaine FRA, Rohner CA, Weeks SJ, Couturier LIE, Bennett MB, Townsend KA, Richardson AJ (2014) Movements and habitat use of reef manta rays off eastern Australia: offshore excursions, deep diving and eddy affinity revealed by satellite telemetry. Mar Ecol Prog Ser 510: 73–86

Kessel ST, Elamin NA, Yurkowski DJ, Chekchak T and others (2017) Conservation of reef manta rays (*Manta alfredi*) in a UNESCO World Heritage Site: large-scale island development or sustainable tourism? PLOS ONE 12:e0185419

Keynes Q (1959) Seychelles, Tropic Isles of Eden. Natl Geogr Mag 116:670–695

Komdeur J, Daan S (2005) Breeding in the monsoon: semi-annual reproduction in the Seychelles warbler (*Acrocephalus sechellensis*). J Ornithol 146:305–313

Lawson JM, Fordham SV, O'Malley MP, Davidson LNK and others (2017) Sympathy for the devil: a conservation strategy for devil and manta rays. PeerJ 5:e3027

Lea JSE (2017) Migratory behaviour and spatial dynamics of large sharks and their conservation implications. PHD dissertation, University of Plymouth

Lea JSE, Humphries NE, von Brandis RG, Clarke CR, Sims DW (2016) Acoustic telemetry and network analysis reveal the space use of multiple reef predators and enhance marine protected area design. Proc R Soc B 283: 20160717

Lenke R (1988) Hormonal control of sleep-appetitive behaviour and diurnal activity rhythms in the cleaner wrasse *Labroides dimidiatus* (Labridae, Teleostei). Behav Brain Res 27:73–85

Letessier TB, Juhel JB, Vigliola L, Meeuwig JJ (2015) Low-cost small action cameras in stereo generates accurate underwater measurements of fish. J Exp Mar Biol Ecol 466:120–126

Marshall AD, Bennett M (2010) The frequency and effect of shark-inflicted bite injuries to the reef manta ray *Manta alfredi*. Afr J Mar Sci 32:573–580

Marshall AD, Compagno LJV, Bennett MB (2009) Redescription of the genus *Manta* with resurrection of *Manta alfredi* (Krefft, 1868) (Chondrichthyes; Myliobatoidei; Mobulidae). Zootaxa 2301:1–28

Marshall AD, Dudgeon CL, Bennett MB (2011) Size and structure of a photographically identified population of

manta rays *Manta alfredi* in southern Mozambique. Mar Biol 158:1111–1124

Marshall AD, Kashiwagi T, Bennett MB, Deakos M and others (2018) *Mobula alfredi* (amended version of 2011 assessment). The IUCN Red List of Threatened Species 2018: e.T195459A126665723

Mathies NH, Ogburn MB, McFall G, Fangman S (2014) Environmental interference factors affecting detection range in acoustic telemetry studies using fixed receiver arrays. Mar Ecol Prog Ser 495:27–38

McCauley DJ, DeSalles PA, Young HS, Papastamatiou YP and others (2014) Reliance of mobile species on sensitive habitats: a case study of manta rays (*Manta alfredi*) and lagoons. Mar Biol 161:1987–1998

Meyer CG, Papastamatiou YP, Clark TB (2010) Differential movement patterns and site fidelity among trophic groups of reef fishes in a Hawaiian marine protected area. Mar Biol 157:1499–1511

Moazzam M (2018) Unprecedented decline in the catches of mobulids: an important component of tuna gillnet fisheries of the Northern Arabian Sea. Working Party on Ecosystems and Bycatch (WPEB). Indian Ocean Tuna Commission. www.iotc.org/documents/unprecedented-decline-catches-mobulids-important-component-tuna-gillnet-fisheries-northern (accessed 27 September 2018)

Musick JA, Burgess G, Cailliet G, Camhi M, Fordham S (2000) Management of sharks and their relatives (Elasmobranchii). Fisheries 25:9–13

Notarbartolo-di-Sciara G (1987) A revisionary study of the genus *Mobula* Rafinesque, 1810 (Chondrichthyes: Mobulidae) with the description of a new species. Zool J Linn Soc 91:1–91

Nøttestad L, Giske J, Holst JC, Huse G (1999) A length-based hypothesis for feeding migrations in pelagic fish. Can J Fish Aquat Sci 56:26–34

O'Malley MP, Townsend KA, Hilton P, Heinrichs S, Stewart JD (2017) Characterization of the trade in manta and devil ray gill plates in China and South-east Asia through trader surveys. Aquat Conserv 27:394–413

O'Shea OR, Kingsford MJ, Seymour J (2010) Tide-related periodicity of manta rays and sharks to cleaning stations on a coral reef. Mar Freshw Res 61:65–73

Papastamatiou YP, Friedlander AM, Caselle JE, Lowe CG (2010) Long-term movement patterns and trophic ecology of blacktip reef sharks (*Carcharhinus melanopterus*) at Palmyra Atoll. J Exp Mar Biol Ecol 386:94–102

Potts GW (1973) The ethology of *Labroides dimidiatus* (Cuv. & Val.) (Labridae, Pisces) on Aldabra. Anim Behav 21: 250–291

R Core Team (2017) R: a language and environment for statistical computing. R Foundation for Statistical Computing, Vienna

Rohner CA, Flam AL, Pierce SJ, Marshall AD (2017) Steep declines in sightings of manta rays and devilrays (Mobulidae) in southern Mozambique. PeerJ Preprints 5:e3051v1. https://doi.org/10.7287/peerj.preprints.3051v1

Schott FA, McCreary JP Jr (2001) The monsoon circulation of the Indian Ocean. Prog Oceanogr 51:1–123

Setyawan E, Sianipar AB, Erdmann MV, Fischer AM and others (2018) Site fidelity and movement patterns of reef manta rays (*Mobula alfredi*: Mobulidae) using passive acoustic telemetry in northern Raja Ampat, Indonesia. NatConserv Res 3:17–31

Sims DW, Witt MJ, Richardson AJ, Southall EJ, Metcalfe JD (2006) Encounter success of free-ranging marine predator movements across a dynamic prey landscape. Proc Biol Sci 273:1195–1201

Stevens GMW (2016) Conservation and population ecology of manta rays in the Maldives. PhD dissertation, University of York

Stevens GMW, Hawkins JP, Roberts CM (2018) Courtship and mating behaviour of manta rays *Mobula alfredi* and *M. birostris* in the Maldives. J Fish Biol 93:344–359

Stewart JD, Beale CS, Fernando D, Sianipar AB, Burton RS, Semmens BX, Aburto-Oropeza O (2016) Spatial ecology and conservation of *Manta birostris* in the Indo-Pacific. Biol Conserv 200:178–183

Stewart JD, Jaine FRA, Armstrong AJ, Armstrong AO and others (2018a) Research priorities to support effective manta and devil ray conservation. Front Mar Sci 5:314

Stewart JD, Nuttall M, Hickerson EL, Johnston MA (2018b) Important juvenile manta ray habitat at Flower Garden Banks National Marine Sanctuary in the northwestern Gulf of Mexico. Mar Biol 165:111

Stoddart DR, Coe MJ, Fosberg FR (1979) D'Arros and St. Joseph, Amirante Islands. Atoll Res Bull 223:1–48

Temple AJ, Kiszka JJ, Stead SM, Wambiji N and others (2018) Marine megafauna interactions with small-scale fisheries in the southwestern Indian Ocean: a review of status and challenges for research and management. Rev Fish Biol Fish 28:89–115

Temple AJ, Wambiji N, Poonian CNS, Jiddawi N, Stead SM, Kiszka JJ, Berggren P (2019) Marine megafauna catch in southwestern Indian Ocean small-scale fisheries from landings data. Biol Conserv 230:113–121

Thorrold SR, Afonso P, Fontes J, Braun CD, Santos RS, Skomal GB, Berumen ML (2014) Extreme diving behaviour in devil rays links surface waters and the deep ocean. Nat Commun 5:4274

Vianna GM, Meekan MG, Meeuwig JJ, Speed CW (2013) Environmental influences on patterns of vertical movement and site fidelity of grey reef sharks (*Carcharhinus amblyrhynchos*) at aggregation sites. PLOS ONE 8:e60331

Ward-Paige CA, Davis B, Worm B (2013) Global population trends and human use patterns of manta and mobula rays. PLOS ONE 8:e74835

Ware DM (1978) Bioenergetics of pelagic fish: theoretical change in swimming speed and ration with body size. J Fish Res Board Can 35:220–228

Weihs D (1973) Optimal fish cruising speed. Nature 245:48

Whitcraft S, O'Malley M, Hilton P (2014) The continuing threat to manta and mobula rays: 2013–14 market surveys, Guangzhou, China. WildAid, San Francisco, CA

White WT, Corrigan S, Yang L, Henderson AC, Bazinet AL, Swofford DL, Naylor GJP (2017) Phylogeny of the manta and devilrays (Chondrichthyes: Mobulidae), with an updated taxonomic arrangement for the family. Zool J Linn Soc 182:50–75

Wickham H (2016) ggplot2: elegant graphics for data analysis. Springer-Verlag, New York, NY

Wood SN (2017) Generalized additive models: an introduction with R. Chapman and Hall/CRC, New York, NY

Editorial responsibility: Elliott Hazen, Pacific Grove, California, USA

Submitted: November 16, 2018; Accepted: May 16, 2019
Proofs received from author(s): June 22, 2019